A comparison of terahertz optical constants and diffusion coefficients of tissue immersion optical clearing agents

Guzel R. Musina[a,b], Arsenii A. Gavdush[a,b], Daria K. Tuchina[a,c], Irina N. Dolganova[b,d], Gennady A. Komandin[a], Sergey V. Chuchupal[a], Olga A. Smolyanskaya[e], Olga P. Cherkasova[a,f,g], Kirill I. Zaytsev[a,b,e], and Valery V. Tuchin[c,e,g,h]

[a]Prokhorov General Physics Institute of the Russian Academy of Sciences, Moscow 119991, Russia
[b]Bauman Moscow State Technical University, Moscow 105005, Russia
[c]Saratov State University, Saratov 410012, Russia
[d]Institute of Solid State Physics of the Russian Academy of Sciences, Chernogolovka 142432, Russia
[e]ITMO University, Saint-Petersburg 199004, Russia
[f]Institute of Laser Physics of Siberian Branch of the Russian Academy of Sciences, Novosibirsk 630090, Russia
[g]Tomsk State University, Tomsk 634050, Russia
[h]Institute of Precision Mechanics and Control of the Russian Academy of Sciences, Saratov 410028, Russia

ABSTRACT

We performed the transmission-mode terahertz (THz) pulsed spectroscopy of several THz-wave penetration-enhancing agents (PEAs): glycerol, propylene glycol, ethylene glycol, and polyethylene glycol, featuring the molecular weight of 200, 300 and 400. We vacuumized the THz beam path in order to reduce an impact of water vapor on measured data. We reconstructed optical properties and dielectric constants of the abovementioned PEAs in the spectral range of 0.1 to 2.5 THz. We analyzed measured THz optical properties along with the literature data for coefficients of PEAs' diffusion into tissues in order to objectively uncover strength and weaknesses of their use in the immersion optical clearing of tissues at THz frequencies.

Keywords: terahertz technology, terahertz biophotonics, terahertz pulsed spectroscopy, optical properties, dielectric constants, immersion optical clearing of tissues, THz-wave penetration-enhancing agents.

1. INTRODUCTION

Recently, methods of THz pulsed spectroscopy and imaging have attracted considerable attention in label-free diagnosis of malignancies with different localization and nosology.[1–4] Particularly, a potential of THz technologies in early noninvasive and intraoperative diagnosis of skin and mucosa cancers,[5–9] least-invasive and intraoperative diagnosis of colon cancers,[10–13] and intraoperative diagnosis of tumors of the breast[14–16] and the brain[17–20] was experimentally demonstrated using THz spectroscopy and imaging of tissues *ex vivo* or *in vivo*. THz pulsed spectroscopy and imaging are among the most widely-applied instruments of THz biophotonics, thanks to an ability for detecting amplitude and phase information about the object response to the applied electromagnetic field in a wide spectral range as a result of a single measurement. Several prototypes of ergonomic, portable and even hand-held devices for medical diagnosis have been developed relying on the principles of the THz pulsed spectroscopy.[21,22]

Despite the attractiveness of THz technology in medical diagnosis, several problems still restrict their transfer to clinical practice; among them:

Further author information:
G.R. Musina, E-mail: guzel-musina12@mail.ru; A.A. Gavdush, E-mail: arsenii.a.gavdush@gmail.com;
K.I. Zaytsev, E-mail: kirzay@gmail.com; V.V. Tuchin, E-mail: tuchinvv@mail.ru.

Saratov Fall Meeting 2018: Optical and Nano-Technologies for Biology and Medicine, edited by Elina A. Genina, Valery V. Tuchin, Proc. of SPIE Vol. 11065, 110651Z · © 2019 SPIE
CCC code: 0277-786X/19/$18 · doi: 10.1117/12.2526168

- high-cost and cumbersomeness of THz instruments;[3]
- absence of both hard waveguides and flexible fibers, which are capable for THz-wave delivery to hardly-accessible tissues and internal organs;[23–25]
- limited spatial resolution of THz spectroscopy and imaging, which prevents accurate delineation of pathology margins;[26–28]
- strong THz-wave absorption by free and bound water, which limits the THz-wave penetration into tissues by hundreds of microns and, thus, yields probing only superficial features of tissues.[3]

It would take significant research and engineering efforts to solve all the abovementioned problems, meanwhile, in this paper, we would focus on the last one.

Recently, several approaches for reducing the THz-wave absorption in tissues have been introduced:

- tissue freezing;[29,30]
- dehydration;[31]
- paraffin-embedding;[18]
- lyophilization;[32]
- immersion optical clearing (IOC).[33–38]

Tissue freezing, dehydration, paraffin-embedding and lyophilization are rather time-consuming, require difficult preparations, and predominantly could not be applied *in vivo*. Furthermore, some of these techniques result in structural changes in tissues during long term exposure. In turn, IOC, which was first introduced in optical range[39–41] and then transferred to THz domain,[33–38] demonstrates rather prominent results. It relies on application of specific chemical THz-wave penetration-enhancing agents (THz-PEAs), which interact with tissues *ex vivo* or *in vivo* and change their optical properties. In optical range, PEA allows for changing the dielectric contrast and extinction coefficient; while, in THz range, it partially substitutes water in tissues, leading to decrease of effective refractive index and absorption coefficient. PEA should be characterised by hyperosmotic status, high diffusion coefficient, and low THz wave absorption. Nevertheless, the lack of data about the THz optical properties of various THz-PEAs does not allow to select the optimal one for applications in THz biophotonics.

In order to mitigate the problem posed by IOC application in the THz range, in this paper, we perform the transmission-mode terahertz (THz) pulsed spectroscopy of several THz-PEAs; among them: glycerol, propylene glycol (PG), ethylene glycol (EG), and polyethylene glycol (PEG) featuring the molecular weight of 200, 300 and 400. We studied optical properties and dielectric constants of these THz-PEAs in the frequency range of 0.1 to 2.5 THz. We analyzed thus measured THz optical properties along with the literature data for coefficients of THz-PEAs' diffusion into tissues. These allows us to objectively uncover strength and weaknesses of these THz-PEAs in the THz IOC of tissues.

2. MATERIALS AND METHODS

2.1 Penetration-enhancing agents

In this study, we used the following set of THz-PEAs without purification:

- glycerol from SpektrChem, Russia;
- PG from Chemical Line, Russia;
- EG from SpektrChem, Russia;
- PEG 200 from Nizhnekamskneftekhim, Russia;
- PEG 300 from Sigma-Aldrich, Germany;
- PEG 400 from Nizhnekamskneftekhim, Russia.

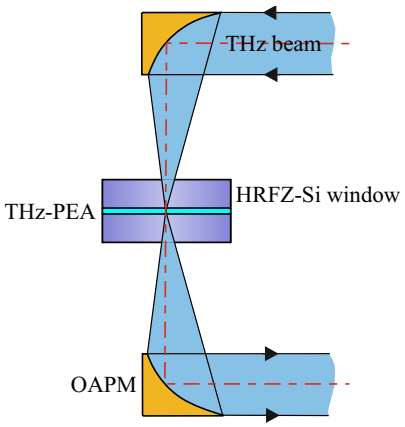

Figure 1. A scheme of the sample chamber and the cuvette for THz pulsed spectroscopy of liquids.

2.2 Experimental setup

In order to study THz-PEAs, we use original THz pulsed spectrometer with LT-GaAs photoconductive antennas and vacuum-capable sample chamber. It operates in transmission mode in the frequency-range of 0.1 to 4.0 THz (when the THz beam path is empty) with the maximal spectral resolution of about 0.015 THz. A scheme of the THz beam path is shown in Fig. 1. When operating with a cuvette for measurements of liquids, the setup provides the spectral operation range of about 0.25 to 2.5 THz due to the THz beam diffraction at the aperture of the sample cuvette, Fresnel losses at its interfaces, as well as THz beam absorption in the volume of media. We use a pair of off-axis parabolic mirrors (OAPM) to focus the THz beam on the sample cuvette and to collimate it after interaction with the sample. In the present work, THz measurements were performed in a vacuum in order to reduce an impact of water vapor absorption on measured data.

As shown in Fig. 1, our sample cuvette is comprised of two windows made of high-resistivity float-zone silicon (HRFZ-Si). Between these windows, we place a THz-PEA layer and a spacer; the latter allows for controlling the thickness of the THz-PEA layer. This sample cuvette and the principles of its operation are described in details in Ref.[38]

2.3 Reconstruction of optical properties

We use a procedure of the THz optical properties reconstruction, which is quite similar to that employed in our previous study.[38] In order to reconstruct the optical properties, we detect reference and sample waveforms of the THz pulsed spectrometer. The reference waveform corresponds to the THz pulse propagating through the sample cuvette with the HRFZ-Si windows placed close to each other – i.e. without the THz-PEA layer and spacer between them; while the sample waveform corresponds to the THz pulse propagating through the cuvette, between the HRFZ-Si windows of which the THz-PEA layer and spacer are trapped.

The HRFZ-Si windows feature considerably larger optical thickness than that of the THz-PEA layer. This feature allows us to filter out a contribution of the satellite pulses, originated owing to multiple THz-wave reflections in the HRFZ-Si windows, from the waveforms of the THz pulsed spectrometer. For this aim, we use the time-domain Tukey apodization (window filter).[42]

The reconstruction procedure is based on the minimization of vector error functional:

$$\widetilde{n}_{\mathrm{s}} = \mathrm{argmin}_{\widetilde{n}_{\mathrm{s}}} \left[\mathbf{\Phi} \right], \qquad \mathbf{\Phi} = \begin{pmatrix} \left| |\widetilde{H}_{\mathrm{exp}}| - |\widetilde{H}_{\mathrm{th}}| \right| \\ \left| \phi\left[\widetilde{H}_{\mathrm{exp}}\right] - \phi\left[\widetilde{H}_{\mathrm{th}}\right] \right| \end{pmatrix}, \tag{1}$$

where $\widetilde{H}_{\mathrm{th}}$ and $\widetilde{H}_{\mathrm{exp}}$ are frequency-dependent theoretical and experimental transfer functions,

$$\widetilde{n} = n' - in'' \equiv n - i\frac{c_0}{4\pi\nu}\alpha \tag{2}$$

is the complex frequency-dependent refractive index of the sample (here, $n \equiv n'$ and n'' stand for the real and imaginary parts of the complex refractive index, α is the frequency-dependent intensity absorption coefficient, and c_0 is the speed of light in free space); $|\ldots|$ and $\phi(\ldots)$ stand for the modulus and the phase operators. Notice, the complex refractive index is related to the complex dielectric permittivity as follows

$$\widetilde{\varepsilon} = \varepsilon' - \varepsilon'' \equiv \widetilde{n}^2, \tag{3}$$

where ε' and ε'' are real and imaginary parts of the complex dielectric permittivity.

The experimental transfer function is defined based on the measured sample $E_{\mathrm{s}}(t)$ and reference $E_{\mathrm{r}}(t)$ waveforms

$$\widetilde{H}_{\mathrm{exp}} = \frac{\mathcal{F}_t\left[E_{\mathrm{s}}(t)\right]}{\mathcal{F}_t\left[E_{\mathrm{r}}(t)\right]} = \frac{\widetilde{E}_{\mathrm{s}}(\nu)}{\widetilde{E}_{\mathrm{r}}(\nu)}, \tag{4}$$

where $\mathcal{F}_t[\ldots]$ is the direct Fourier transform operator. The theoretical transfer function describes propagation of the reference and sample pulses through the layered media including the THz beam splitting at the interfaces, as well as its phase delays in bulk media; it is defined as follows

$$\widetilde{H}_{\mathrm{th}} = \widetilde{T}_{1,2}\widetilde{T}_{2,1}\frac{\widetilde{P}_2(l_2)}{\widetilde{P}_0(l_2)}\sum_{j=0}^{N}(\widetilde{P}_2(l_2)\widetilde{R}_{2,1})^{2j}, \tag{5}$$

where indices 0, 1 and 2 stand for the free space, HRFZ-Si and THz-PEA media, respectively.

The THz-wave interaction with the interfaces of the sample cuvette is described by the Fresnel formulas for the normal incidence; they define transmission and reflection of the THz wave at the interface between m^{th} and k^{th} media:

$$\widetilde{T}_{\mathrm{m,k}} = \frac{2\widetilde{n}_{\mathrm{m}}}{\widetilde{n}_{\mathrm{m}} + \widetilde{n}_{\mathrm{k}}}, \qquad \widetilde{R}_{\mathrm{m,k}} = \frac{\widetilde{n}_{\mathrm{m}} - \widetilde{n}_{\mathrm{k}}}{\widetilde{n}_{\mathrm{m}} + \widetilde{n}_{\mathrm{k}}}, \tag{6}$$

where $\widetilde{n}_{\mathrm{m}}$ and $\widetilde{n}_{\mathrm{k}}$ stand for the complex refractive indices of the two media. In turn, the modified Bouguer-Lambert-Beer law describes the phase delay and absorption of THz wave in a q^{th} medium

$$\widetilde{P}(\widetilde{n}_{\mathrm{q}}, l_{\mathrm{q}}) = \exp\left(-i\frac{2\pi\nu}{c}\widetilde{n}_{\mathrm{q}}l_{\mathrm{q}}\right), \tag{7}$$

where $\widetilde{n}_{\mathrm{q}}$ and l_{q} stand for the complex refractive index and the length of this medium. Notice, the complex refractive indices of the free space $\widetilde{n}_0$ and HRFZ-Si $\widetilde{n}_1$, and the equal thickness of the reference windows l_1 are known *a priori*; while the complex refractive index of THz-PEA $\widetilde{n} \equiv \widetilde{n}_2$ is determined via Eq. (1).

3. RESULTS

We applied the described method for studying the THz optical properties of the abovementioned THz-PEAs. In Fig. 2, we show the optical properties of all considered THz-PEAs in the frequency range of 0.2 and 2.5 THz. For each of the considered THz-PEAs, we measured the THz response of samples with different thickness, ranging between 80 and 500 μm. This yields selection of the optimal thickness, providing simultaneously a broadband transmission of the sample and an appropriate sensitivity of measurements in the entire frequency range. In Fig. 2, we show the error bars representing the maximal possible errors within the considered spectral range; this error is assumed to be equal for all examined THz-PEAs. In this figure, we also show, in yellow, the low frequency range between 0.2 and 0.25 THz, where distortions of the data due to diffraction effects are expected. The obtained results are in a good agreement with our previous data,[38] measured in a less broad spectral range using the THz pulsed spectrometer without vacuumization of the THz beam path. From Fig. 2, we notice that the lowest THz-wave absorption is observed for PEG 300 and PEG 400, making them promising potential candidates for tissue IOC at THz frequencies from the viewpoint of THz-wave penetration depth enhancement.

At the same time, for selection of the optimal THz-PEAs, it is important to take into account their diffusion coefficients D for various types of biological tissues and organs – namely, larger D would provide faster diffusion process, reducing the duration of IOC procedure.[41] In order to simultaneously account the THz-wave absorption

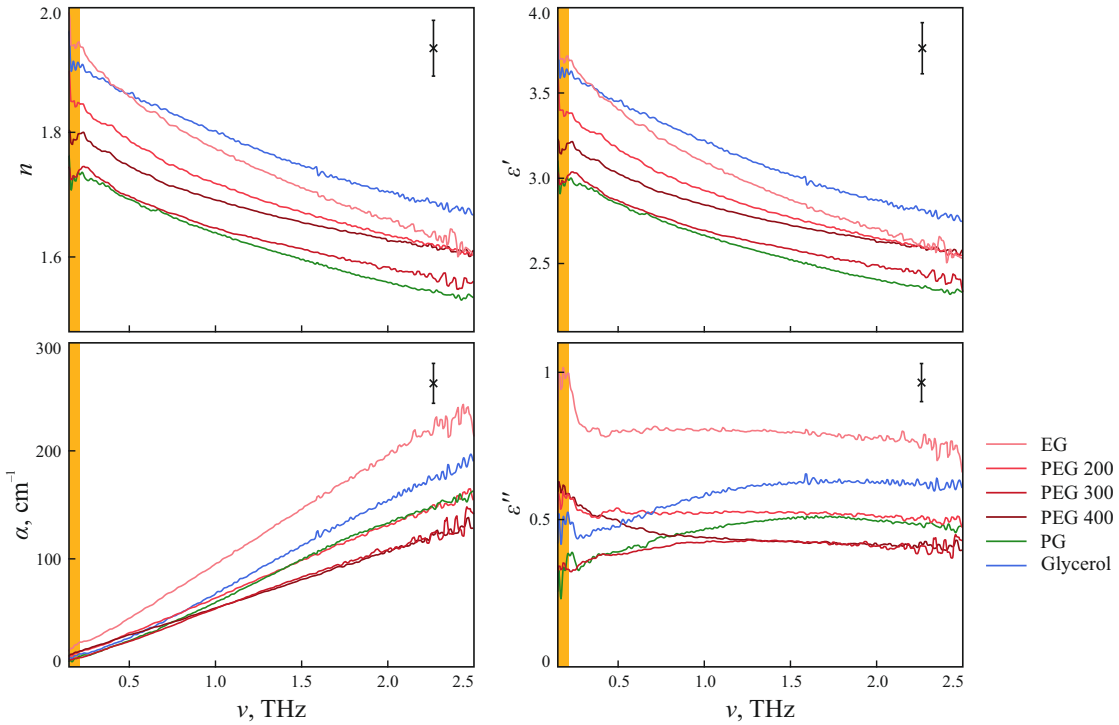

Figure 2. Optical properties and dielectric constants of the considered THz-PEAs in the frequency range between 0.2 and 2.5 THz. The error bars represent 3σ confidential interval of measurements. At low frequencies, we show, in yellow, the spectral range where we could expect distortions of the data caused by the THz-beam diffraction on the cuvette aperture.

coefficient and diffusion coefficients, we take D from the well-known literature data. Particularly, from the Refs.,[36,41,43–47] we can find D for all considered THz-PEAs, except PEG 200, for various types of biological media exposed to IOC. Then, the coefficient of PEG 200 diffusion in water was calculated relying on the following equation from the Ref.[48]

$$D_0\left(M_\mathrm{w}\right) = 7 \times 10^{-9} M_\mathrm{w}^{-0.46}. \tag{8}$$

In Table 1, we summarized the literature data on THz-PEA diffusion coefficients. In Fig. 3, we show diagrams illustrating the data on THz-wave absorption coefficients and diffusion coefficients of THz-PEAs in various biological tissues: (a), (b), and (c) correspond to THz-PEAs' diffusion in water, rat skin, and muscles *ex vivo*, correspondingly. In these diagrams, the horizontal axis represents D, while the vertical axis represents α at

Table 1. THz-PEA diffusion coefficients in water, rat skin, and muscles *ex vivo*.

Tissue	PEA	Diffusion coefficient ×10^{-6}, cm^2 /s	Ref.
Water	PEG 200	6.12	Eq. (7) [48]
	PEG 300	5.08	[44]
	PEG 400	4.45	[44]
	PG	12.30	[45]
	EG	12.20	[46]
	Glycerol	9.30	[43]
Rat skin *ex vivo*	PEG 300	1.830 ± 2.220	[41]
	PEG 400	1.700 ± 1.470	[41]
	PG	0.135 ± 0.095	[41]
	Glycerol	3.230 ± 2.210	[41]
Muscle tissue *ex vivo*	EG	0.46	[47]
	PG	2.00	[36]
	Glycerol	2.90	[36]

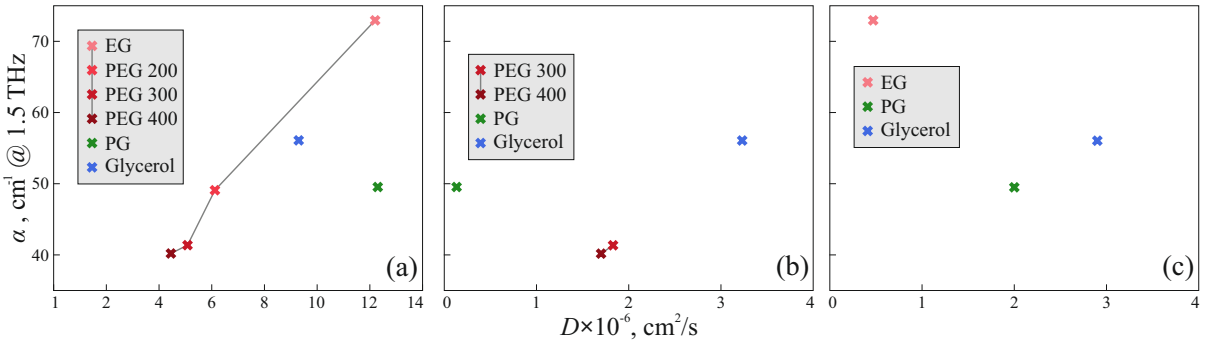

Figure 3. A comparison of THz-PEAs based on the measured THz wave absorption coefficient α at 1.5 THz and the literature data on coefficients D of their diffusion (a) in water, (b) in rat skin tissues *ex vivo*, and (c) in muscle tissues *ex vivo*. In (a) and (b), the markers for EG and PEG featuring different molecular weight are connected with gray solid line for clarity.

1.5 THz; here, for simplicity, we considered α at the particular frequency.

From Fig. 3, we observe that despite PEG 300 and PEG 400 are characterized with the lowest THz-wave absorption (among the considered THz-PEAs), they also feature low diffusion coefficients, which could make their use for IOC of tissues sub-optimal due to long terms of clearing procedure. In turn, despite EG possesses high diffusion coefficient (in water), it feature the highest THz-wave absorption (among the considered THz-PEAs) and low diffusion rate in rat muscle,[47] results in non-attractive usage of this THz-PEA use in IOC of tissues at THz frequencies. As compared to PEG 300 and PEG 400, the THz-wave absorption coefficients of PG and glycerol is 20–30% higher, while their diffusion coefficients are several times higher; thus, PG and glycerol could be applied for IOC of tissues at THz frequencies for achieving a compromise between the THz-wave penetration depth enhancement and the duration of clearing procedure.

It is important to notice that, in Table 1 and Fig. 3, we present a literature data for predominantly the effective diffusion coefficients of the THz-PEAs in tissue, which has the intermediate value between the diffusion coefficients of pure agent (slow process) and of water (fast process). In turn, the considered diffusion coefficient of EG in muscle *ex vivo* (0.46×10^{-6} cm^2/s) corresponds to that of pure THz-PEA[47] (therefore, it is lower than that of other THz-PEAs), while the corresponding diffusion coefficient of water in Ref.[47] is 3.12×10^{-6} cm^2/s. Since water is a dominant absorber of THz radiation in tissues,[3] and its diffusion coefficient seems to be more important parameter for the THz-wave penetration depth enhancement, in future studies, it would be optimal to perform separate analysis of diffusion coefficients for pure THz-PEA and water, paying significant attention to behaviour of water during clearing process.

Evidently, the considered approach for selection of optical THz-PEA for IOC of tissues at THz frequencies reveals an interplay between the THz-wave penetration enhancement and the duration of clearing process. Depending on the particular application of IOC in THz biophotonics, one could select different THz-PEAs (or even their mixtures) in order to achieve the desired performance. Finally, we should stress that, in this study, we considered a limited number of THz-PEAs, as well as few types of biological tissues. Therefore, a full-blown study, involving the use of larger amount of THz-PEAs and different biological objects (both *ex vivo* and *in vivo*) is required in order to analyze potential of IOC in THz range, as well as to select optimal THz-PEAs for particular applications of THz technology.

4. CONCLUSIONS

In this paper, we have studied the THz optical properties and dielectric constants of different THz-PEAs (glycerol, PG, EG, PEG 200, PEG 300, PEG 400) using the THz pulsed spectroscopy. We analyzed thus measured THz optical properties simultaneously with the literature data for coefficients of THz-PEAs' diffusion in biological tissues. The observed results allows us for selecting optimal THz-PEAs (among the considered ones) for IOC of tissues in the THz range.

ACKNOWLEDGMENTS

Development of the cuvette and spectroscopic measurements by G.R. Musina, D.K. Tuchina, G.A. Komandin, S.V. Chuchupal, and O.P. Cherkasova, were supported by the Russian Science Foundation, Project # 18–12–00328. Reconstruction of the dielectric response of THz-PEAs by O.A. Smolyanskaya, and K.I. Zaytsev was supported by the Russian Foundation for Basic Research (RFBR), Project # 18–51–16002. Analysis of experimental and literature data on absorption and diffusion coefficients by V.V. Tuchin was supported by RFBR, Project # 18–52–16025.

REFERENCES

[1] Yang, X., Zhao, X., Yang, K., Liu, Y., Liu, Y., Fu, W., and Luo, Y., "Biomedical applications of terahertz spectroscopy and imaging," *Trends in Biotechnology* **34**(10), 810–824 (2016).

[2] Sun, Q., He, Y., Liu, K., Fan, S., Parrott, E., and Pickwell-MacPherson, E., "Recent advances in terahertz technology for biomedical applications," *Quantitative Imaging in Medicine and Surgery* **7**(3), 345–355 (2017).

[3] Smolyanskaya, O., Chernomyrdin, N., Konovko, A., Zaytsev, K., Ozheredov, I., Cherkasova, O., Nazarov, M., Guillet, J.-P., Kozlov, S., Kistenev, Y., Coutaz, J.-L., Mounaix, P., Vaks, V., Son, J.-H., Cheon, H., Wallace, V., Feldman, Y., Popov, I., Yaroslavsky, A., Shkurinov, A., and Tuchin, V., "Terahertz biophotonics as a tool for studies of dielectric and spectral properties of biological tissues and liquids," *Progress in Quantum Electronics* **62**, 1–77 (2018).

[4] Guerboukha, H., Nallappan, K., and Skorobogatiy, M., "Toward real-time terahertz imaging," *Advances in Optics and Photonics* **10**(4), 843–938 (2018).

[5] Woodward, R., Wallace, V., Pye, R., Cole, B., Arnone, D., Linfield, E., and Pepper, M., "Terahertz pulse imaging of *ex vivo* basal cell carcinoma," *Journal of Investigative Dermatology* **120**(1), 72–78 (2003).

[6] Wallace, V., Fitzgerald, A., Shankar, S., Flanagan, N., Pye, R., Cluff, J., and Arnone, D., "Terahertz pulsed imaging of basal cell carcinoma *ex vivo* and *in vivo*," *British Journal of Dermatology* **151**(2), 424–432 (2004).

[7] Joseph, C., Patel, R., Neel, V., Giles, R., and Yaroslavsky, A., "Imaging of *ex vivo* nonmelanoma skin cancers in the optical and terahertz spectral regions. Optical and terahertz skin cancers imaging," *Journal of Biophotonics* **7**(5), 295–303 (2014).

[8] Zaytsev, K., Kudrin, K., Karasik, V., Reshetov, I., and Yurchenko, S., "*In vivo* terahertz spectroscopy of pigmentary skin nevi: Pilot study of non-invasive early diagnosis of dysplasia," *Applied Physics Letters* **106**(5), 053702 (2015).

[9] Sim, Y., Park, J., Ahn, K.-M., Park, C., and Son, J.-H., "Terahertz imaging of excised oral cancer at frozen temperature," *Biomedical Optics Express* **4**(8), 1413–1421 (2013).

[10] Reid, C., Fitzgerald, A., Reese, G., Goldin, R., Tekkis, P., OKelly, P., Pickwell-MacPherson, E., Gibson, A., and Wallace, V., "Terahertz pulsed imaging of freshly excised human colonic tissues," *Physics in Medicine and Biology* **56**(14), 4333–4353 (2011).

[11] Doradla, P., Alavi, K., Joseph, C., and Giles, R., "Detection of colon cancer by continuous-wave terahertz polarization imaging technique," *Journal of Biomedical Optics* **18**(9), 090504 (2013).

[12] Hou, D., Li, X., Cai, J., Ma, Y., Kang, X., Huang, P., and Zhang, G., "Terahertz spectroscopic investigation of human gastric normal and tumor tissues," *Physics in Medicine and Biology* **59**(18), 5423–5440 (2014).

[13] Doradla, P., Joseph, C., and Giles, R., "Terahertz endoscopic imaging for colorectal cancer detection: Current status and future perspectives," *World Journal of Gastrointestinal Endoscopy* **9**(8), 346–358 (2017).

[14] FitzGerald, A., Wallace, V., Jimenez-Linan, M., Bobrow, L., Pye, R., Purushotham, A., and Arnone, D., "Terahertz pulsed imaging of human breast tumors," *Radiology* **239**(2), 533–540 (2006).

[15] Ashworth, P.C. anda Pickwell-MacPherson, E., Provenzano, E., Pinder, S., Purushotham, A., Pepper, M., and Wallace, V., "Terahertz pulsed spectroscopy of freshly excised human breast cancer," *Optics Express* **17**(15), 12444–12454 (2009).

[16] Truong, B., Tuan, H., Fitzgerald, A., Wallace, V., and Nguyen, H., "A dielectric model of human breast tissue in terahertz regime," *IEEE Transactions on Biomedical Engineering* **62**(2), 699–707 (2015).

[17] Oh, S., Kim, S.-H., Ji, Y., Jeong, K., Park, Y., Yang, J., Park, D., Noh, S., Kang, S.-G., Huh, Y.-M., Son, J.-H., and Suh, J.-S., "Study of freshly excised brain tissues using terahertz imaging," *Biomedical Optics Express* **5**(8), 2837–2842 (2014).

[18] Meng, K., Chen, T.-N., Chen, T., Zhu, L.-G., Liu, Q., Li, Z., Li, F., Zhong, S.-C., Li, Z.-R., Feng, H., and Zhao, J.-H., "Terahertz pulsed spectroscopy of paraffin-embedded brain glioma," *Journal of Biomedical Optics* **19**(7), 077001 (2014).

[19] Ji, Y., Oh, S., Kang, S.-G., Heo, J., Kim, S.-H., Choi, Y., Song, S., Son, H., Kim, S., Lee, J., Haam, S., Huh, Y., Chang, J., Joo, C., and Suh, J.-S., "Terahertz reflectometry imaging for low and high grade gliomas," *Scientific Reports* **6**, 36040 (2016).

[20] Gavdush, A., Chernomyrdin, N., Malakhov, K., Beshplav, S.-I., Dolganova, I., Kosyrkova, A., Nikitin, P., Musina, G., Katyba, G., Reshetov, I., Cherkasova, O., Komandin, G., Karasik, V., Potapov, A., Tuchin, V., and Zaytsev, K., "Terahertz spectroscopy of gelatin-embedded human brain gliomas of different grade: A road toward the intraoperative thz diagnosis," *Journal of Biomedical Optics* (2018, Under Review).

[21] Echchgadda, I., Grundt, J., Tarango, M., Ibey, B., Tongue, T., Liang, M., Xin, H., and Wilmink, G., "Using a portable terahertz spectrometer to measure the optical properties of *in vivo* human skin," *Journal of Biomedical Optics* **18**(12), 120503 (2013).

[22] Grootendorst, M., Fitzgerald, A., Brouwer de Koning, S., Santaolalla, A., Portieri, A., Van Hemelrijck, M., Young, M., Owen, J., Cariati, M., Pepper, M., Wallace, V., Pinder, S., and Purushotham, A., "Use of a handheld terahertz pulsed imaging device to differentiate benign and malignant breast tissue," *Biomedical Optics Express* **8**(6), 2932–2945 (2017).

[23] Zaytsev, K., Katyba, G., Kurlov, V., Shikunova, I., Karasik, V., and Yurchenko, S., "Terahertz photonic crystal waveguides based on sapphire shaped crystals," *IEEE Transactions on Terahertz Science and Technology* **6**(4), 576–582 (2016).

[24] Katyba, G., Zaytsev, K., Chernomyrdin, N., Shikunova, I., Komandin, G., Anzin, V., Lebedev, S., Spektor, I., Karasik, V., Yurchenko, S., Reshetov, I., Kurlov, V., and Skorobogatiy, M., "Sapphire photonic crystal waveguides for terahertz sensing in aggressive environments," *Advanced Optical Materials* **6**(22), 1800573 (2018).

[25] Katyba, G., Zaytsev, K., Dolganova, I., Shikunova, I., Chernomyrdin, N., Yurchenko, S., Komandin, G., Reshetov, I., Nesvizhevsky, V., and Kurlov, V., "Sapphire shaped crystals for waveguiding, sensing and exposure applications," *Progress in Crystal Growth and Characterization of Materials* **64**(4), 133–151 (2018).

[26] Fan, B., Neel, V., and Yaroslavsky, A., "Multimodal imaging for nonmelanoma skin cancer margin delineation," *Lasers in Surgery and Medicine* **49**(3), 319–326 (2017).

[27] Chernomyrdin, N., Frolov, M., Lebedev, S., Reshetov, I., Spektor, I., Tolstoguzov, V., Karasik, V., Khorokhorov, A., Koshelev, K., Schadko, A., Yurchenko, S., and Zaytsev, K., "Wide-aperture aspherical lens for high-resolution terahertz imaging," *Review of Scientific Instruments* **88**(1), 014703 (2017).

[28] Chernomyrdin, N., Kucheryavenko, A., Kolontaeva, G., Katyba, G., Dolganova, I., Karalkin, P., Ponomarev, D., Kurlov, V., Reshetov, I., Skorobogatiy, M., Tuchin, V., and Zaytsev, K., "Reflection-mode continuous-wave 0.15λ-resolution terahertz solid immersion microscopy of soft biological tissues," *Applied Physics Letters* **113**(11), 111102 (2018).

[29] Hoshina, H., Hayashi, A., Miyoshi, N., Miyamaru, F., and Otani, C., "Terahertz pulsed imaging of frozen biological tissues," *Applied Physics Letters* **94**(12), 123901 (2009).

[30] Sim, Y., Ahn, K.-M., Park, J., Park, C.-S., and Son, J.-H., "Temperature-dependent terahertz imaging of excised oral malignant melanoma," *IEEE Transactions on terahertz science and technology* **3**(4), 368–373 (2013).

[31] He, Y., Liu, K., Au, C., Sun, Q., Parrott, E., and PickWell-MacPherson, E., "Determination of terahertz permittivity of dehydrated biological samples," *Physics in Medicine and Biology* **62**(23), 8882–8893 (2017).

[32] Png, G., Choi, J., Ng, B.-H., Mickan, S., Abbott, D., and Zhang, X.-C., "The impact of hydration changes in fresh bio-tissue on THz spectroscopic measurements," *Physics in Medicine and Biology* **53**(13), 3501–3517 (2008).

[33] Oh, S., Kim, S.-H., Jeong, K., Park, Y., Huh, Y.-M., Son, J.-H., and Suh, J.-S., "Measurement depth enhancement in terahertz imaging of biological tissues," *Optics Express* **21**(18), 21299–21305 (2013).

[34] Kolesnikov, A., Kolesnikova, E., Kolesnikova, K., Tuchina, D., Popov, A., Skaptsov, A., Nazarov, M., Shkurinov, A., Terentyuk, A., and Tuchin, V., "THz monitoring of the dehydration of biological tissues affected by hyperosmotic agents," *Physics of Wave Phenomena* **22**(3), 169–176 (2014).

[35] Kolesnikov, A., Kolesnikova, E., Tuchina, D., Terentyuk, A., Nazarov, M., Skaptsov, A., Shkurinov, A., and Tuchin, V., "*In vitro* terahertz spectroscopy of rat skin under the action of dehydrating agents," *Proceedings of SPIE* **9031**, 90310D (2014).

[36] Kolesnikov, A., Kolesnikova, E., Popov, A., Nazarov, M., Shkurinov, A., and Tuchin, V., "*In vitro* terahertz monitoring of muscle tissue dehydration under the action of hyperosmotic agents," *Quantum Electronics* **44**(7), 633–640 (2014).

[37] Smolyanskaya, O., Schelkanova, I., Kulya, M., Odlyanitskiy, E., Goryachev, I., Tcypkin, A., Grachev, Y., Toropova, Y., and Tuchin, V., "Glycerol dehydration of native and diabetic animal tissues studied by THz-TDS and NMR methods," *Biomedical Optics Express* **9**(3), 1198–1215 (2018).

[38] Musina, G., Dolganova, I., Malakhov, K., Gavdush, A., Chernomyrdin, N., Tuchina, D., Komandin, G., Chuchupal, S., Cherkasova, O., Zaytsev, K., and Tuchin, V., "Terahertz spectroscopy of immersion optical clearing agents: DMSO, PG, EG, PEG," *Proceedings of SPIE* **10800**, 108000F (2018).

[39] Tuchin, V., [*Tissue Optics: Light Scattering Methods and Instruments for Medical Diagnosis: Third Edition*], SPIE (2015).

[40] Genina, E., Bashkatov, A., Sinichkin, Y., Yanina, I., and Tuchin, V., "Optical clearing of biological tissues: Prospects of application in medical diagnostics and phototherapy," *Journal of Biomedical Photonics and Engineering* **1**(1), 22–58 (2015).

[41] Bashkatov, A., Berezin, K., Dvoretskiy, K., Chernavina, M., Genina, E., Genin, V., Kochubey, V., Lazareva, E., Pravdin, A., Shvachkina, M., Timoshina, P., Tuchina, D., Yakovlev, D., Yakovlev, D., Yanina, I., Zhernovaya, O., and Tuchin, V., "Measurement of tissue optical properties in the context of tissue optical clearing," *Journal of Biomedical Optics* **23**(9), 091416 (2018).

[42] Zaytsev, K., Gavdush, A., Lebedev, S., Karasik, V., and Yurchenko, S., "A method of studying spectral optical characteristics of a homogeneous medium by means of terahertz time-domain spectroscopy," *Optics and Spectroscopy* **118**(4), 552–562 (2015).

[43] Hayduk, W. and Laudie, H., "Prediction of diffusion coefficients for nonelectrolytes in dilute aqueous solutions," *AlChE Journal* **20**(3), 611–615 (1974).

[44] Tuchina, D., Genin, V., Bashkatov, A., Genina, E., and Tuchin, V., "Optical clearing of skin tissue *ex vivo* with polyethylene glycol," *Optics and Spectroscopy* **120**(1), 36–45 (2016).

[45] Web-site of Contact GSI Environmental Inc., URL: https://www.gsi-net.com/en/publications/gsi-chemical-database/single/469.html.

[46] Web-site of Contact GSI Environmental Inc., URL: https://www.gsi-net.com/en/publications/gsi-chemical-database/single/276-CAS-107211.html.

[47] Oliveira, L., Carvalho, M., Nogueira, M., and Tuchin, V., "Diffusion characteristics of ethylene glycol in skeletal muscle," *Journal of Biomedical Optics* **20**(5), 051019 (2015).

[48] Johansson, L., Skantze, U., and Lofroth, J.-E., "Diffusion and interaction in gels and solutions. 2. Experimental results on the obstruction effect," *Macromolecules* **24**(22), 6019–6023 (1991).